Free Radical Biology and Medicine 172 (2021) 298–311

Contents lists available at ScienceDirect

Free Radical Biology and Medicine

journal homepage: www.elsevier.com/locate/freeradbiomed

Original article

DNA damage and oxidant stress activate p53 through differential upstream signaling pathways

Tao Shi [a], Daan M.K. van Soest [a], Paulien E. Polderman [a], Boudewijn M.T. Burgering [a,b], Tobias B. Dansen [a,*]

[a] Center for Molecular Medicine, Molecular Cancer Research, the Netherlands
[b] Oncode Institute, University Medical Center Utrecht, Universiteitsweg, 100 3584, CG, Utrecht, the Netherlands

ARTICLE INFO

Keywords:
Oxidative signaling
DNA damage Response
p53 activation
p38MAPK
Stress activated protein kinases

ABSTRACT

Stabilization and activation of the p53 tumor suppressor are triggered in response to various cellular stresses, including DNA damaging agents and elevated Reactive Oxygen Species (ROS) like H_2O_2. When cells are exposed to exogenously added H_2O_2, ATR/CHK1 and ATM/CHK2 dependent DNA damage signaling is switched on, suggesting that H_2O_2 induces both single and double strand breaks. These collective observations have resulted in the widely accepted model that oxidizing conditions lead to DNA damage that subsequently mediates a p53-dependent response like cell cycle arrest and apoptosis. However, H_2O_2 also induces signaling through stress-activated kinases (SAPK, e.g., JNK and p38 MAPK) that can activate p53. Here we dissect to what extent these pathways contribute to functional activation of p53 in response to oxidizing conditions. Collectively, our data suggest that p53 can be activated both by SAPK signaling and the DDR independently of each other, and which of these pathways is activated depends on the type of oxidant used. This implies that it could in principle be possible to modulate oxidative signaling to stimulate p53 without inducing collateral DNA damage, thereby limiting mutation accumulation in both healthy and tumor tissues.

1. Introduction

P53 transcriptional activity induces a wide range of cellular processes including cell cycle arrest, DNA damage repair, senescence, apoptosis and metabolism. Collectively these programs ensure genome integrity, lower the chance to pass on DNA mutations down the lineage and hence provide tumor suppressive function. Nevertheless, p53-dependent programs such as transient cell cycle arrest and the regulation of metabolism can also function to support cell survival, for instance upon nutrient depletion, by providing means to maintain cellular energy levels and control redox balance [1].

Under basal, unstressed conditions p53 activity is low as a result of the continuous turnover of the p53 protein, which is under control of MDM2 dependent poly-ubiquitinylation and subsequent proteasomal degradation. Stabilization of p53 is the outcome of several cellular stress signaling pathways. Upon DNA double strand breaks, ATM undergoes activating autophosphorylation and phosphorylates p53 on Ser15, but also activates CHK2 which in turn phosphorylates p53 on Ser20 [2,3]. These two phosphorylation events facilitate p53 stabilization by preventing MDM2-mediated p53 ubiquitinylation and subsequent proteasomal degradation [4]. In addition to ATM kinase, two members of the stress-activated protein kinase (SAPK) family: *c*-Jun N-terminal kinase (JNK) and p38 MAPK have also been shown to mediate p53 activation in response to UV irradiation, some chemotherapeutic agents but also upon exposure to Reactive Oxygen Species like H_2O_2, all of which also have been shown to induce DNA damage [5–7]. JNK phosphorylates p53 on Ser20 and Thr81 [8,9], whereas p38 MAPK has been implicated in phosphorylation on Ser15, 33, 37 and 46 [5,7]. Because JNK and p38 MAPK are both proline-directed Ser/Thr protein kinases, it may be difficult to distinguish whether and which of these kinases specifically target a certain site. In any case, these PTMs also induce p53 stabilization and transcriptional activity.

As mentioned, many treatments that engage the cellular DNA damage response also activate SAPK signaling and *vice versa*. It is therefore often difficult to pinpoint which of these pathways is the predominant activator of p53 [10,11]. For Reactive Oxygen Species (ROS), such as superoxide anions ($O_2^{\bullet-}$), hydroxyl radicals ($HO^{\bullet}$) and hydrogen peroxide (H_2O_2), the classical view is that these indeed contribute to damage to

* Corresponding author.
E-mail address: t.b.dansen@umcutrecht.nl (T.B. Dansen).

https://doi.org/10.1016/j.freeradbiomed.2021.06.013
Received 14 April 2021; Received in revised form 28 May 2021; Accepted 13 June 2021
Available online 16 June 2021

proteins, lipids and DNA [12,13]. Exogenously added H_2O_2 indeed induces both the DNA damage response pathways associated with single and double DNA breaks [14–16]. Based on these observations it has been suggested that H_2O_2 that is generated endogenously as a consequence of for instance mitochondrial respiration can directly contribute to mutations in genomic DNA, and therefore could be a driver of aging and tumor initiation and progression [17,18].

In the literature various terms (e.g. oxidative stress, redox signaling) for signaling in response to elevated ROS are being used. For a clear definition we would like to refer to the review by Sies and Jones [12], in which the authors discriminate between oxidative eu-stress and oxidative distress, depending on the levels of H_2O_2. The term Redox signaling is mostly associated with physiological H_2O_2 levels and specific signaling that is regulated through reversible cysteine oxidation, whereas oxidative distress may result from random oxidative damage to cellular constituents including the DNA, leading to induction of the DNA damage response (DDR) through activation of ATM and ATR. However, it is not always clear where the border between eustress and distress lies. In this study we compared and dissected effects that are triggered in response to treatment with oxidants and DNA-damaging agents, to model and dissect what happens during therapeutic activation of p53. Because in most cases the concentration of oxidants used is well above what would be considered to occur endogenously, we have opted to use the term 'oxidative signaling' for the observed responses downstream of exposure to oxidants that trigger signaling as measured by i.e. SAPK activation, to distinguish it from the oxidant-induced DDR as well as from redox signaling under physiological levels of ROS.

ROS induced SAPK activation indeed occurs independent of DNA damage as a result of oxidative signaling through the reversible oxidation of protein cysteine-thiols [12]. H_2O_2 leads for instance to disulfide-dependent dimerization and activation of ASK-1, which activates JNK and p38 MAPK followed by p53 stabilization [19,20]. To complicate things further, ATM has also been reported to be activated by cysteine oxidation independent of DNA DSBs [21]. Taken together, and as we recently outlined in detail [10], it remains unclear which upstream signaling pathways (ATM, JNK and p38 MAPK) are responsible for oxidant-induced p53 activation in response to which signaling pathways (DNA damage or oxidative signaling, or both) and to what extent.

In the present study, we aim to dissect signaling cascades upstream of p53 in response to DNA damage signaling and oxidative signaling. We show that p53 activation in response to DNA damage is mainly mediated by the ATM kinase, whereas oxidative signaling-mediated p53 activation depends mostly on p38 MAPK and is independent of the ATM-dependent DNA damage response. ATM, JNK and p38 MAPK are all activated by H_2O_2, but only ATM and JNK are required for H_2O_2-induced p53 activation. The thiol oxidant diamide activates both JNK and p38 MAPK but not ATM, and p53 activation by diamide depends on p38 MAPK. Collectively, we show that functional p53 activation by oxidative signaling and DNA damage is mediated by distinct signaling pathways. Our observations imply that for therapeutic strategies p53 can in principle be reactivated by oxidative signaling without collateral DNA damage, lowering the chance of inducing mutations that drive tumor progression or initiate new malignancies in healthy neighboring tissue.

2. Materials and methods

2.1. Reagents and antibodies

5-Fluorouracil (5-FU), Etoposide, Diamide, H_2O_2, Neocarzinostatin (NCS), Auranofin (AFN) and ATM inhibitor (KU55933) were from Sigma. Oxaliplatin, Doxorubicin, Mitomycin C, JNK inhibitor (SP600126) and p38 MAPK inhibitor (PH797804) were from Bio-Connect Life Sciences. Nutlin-3a was from Sanbio.

Antibodies were used as follows: CHK2(A-11), CHK1(G-4), p53 (DO-1), p21 (M − 19), JNK (D-2) and *c*-Jun (SC-1694) were from Santa Cruz Biotechnology. ATM(D2E2), pp53(Ser15) (CS9286), pCHK2(Thr68) (CS2661), pCHK1(S345) (CS2348), p-C-Jun (Ser63) (CS9261), pJNK (Thr183/Tyr185) (CS9251), p38 MAPK(CS9212), pp38 MAPK (Thr180/Tyr182) (CS4511), pATF-2 (Thr71) (CS24329) and pERK1/2 (T202/Y204) (CS4370) were from Cell Signaling Technology. Phospho-Histone H2AX (Ser139) and GAPDH (MAB374) were from EMD Millipore. pATM (Ser1981) (ab81292) from abcam. HRP or fluorescently labeled secondary antibodies were used for detection on Western blot.

2.2. Cell culture

Non-small-cell-lung cancer cells (NCI–H1299, ATCC® CRL-5803™) [22] cells were cultured in DMEM high-glucose (4,5 g/L) supplemented with 10% FBS, 2 mM L-glutamine and 100 Units Penicillin-Streptomycin (All from Sigma Aldrich). RPE^{Tert} and RPE^{Tert} p53-KO cells (a gift from dr. René Medema [23]**)** were cultured in DMEM/F-12 high-glucose supplemented with 10% FBS and 100 U Penicillin-Streptomycin (Sigma Aldrich). All cell types were cultured at 37 °C under a 6% CO_2 atmosphere. Cell transfection was carried out using PEI (Sigma Aldrich).

2.3. Plasmids and lentiviral transduction

Plasmids containing the sequences for HyPer7-NLS and HyPer7-NES were a kind gift from Dr. Vsevolod Belousov [24]. The HyPer7-NLS and -NES sequences were cloned into a modified form of the lentiviral backbone pLV-H2B-mNeon-ires-Puro, where the puromycin resistance cassette was replaced by a blasticidin resistance gene [25,26] by infusion cloning using primers designed in SnapGene software **(See** Table S1**)**. The PCR products were isolated from a 1% agarose gel using a gel extraction kit (Qiagen). The PCR products were ligated into the linearized backbone (digested with *Bst*BI and *Nhe*I, New England Biolabs) using the In-Fusion HD cloning kit (Takara), according to manufacturer's protocol. Lentiviral HyPer7-NLS and HyPer7-NES constructs were transfected into HEK293T cells together with third-generation packaging vectors. Virus was purified from filtered media (0.45 μm) by ultracentrifugation and RPE^{Tert} cells were infected and selected with Blasticidin (20 μg/ml, Bio connect). The correct localization of the HyPer7-NLS and -NES proteins was confirmed by fluorescence microscopy (Fig. 1A, C).

pDONR223-p53-WT plasmid was a gift form Jesse Boehm & William Hahn & David Root (Addgene plasmid # 81,754 [27]). The p53 triple cysteine mutant (C182S, C229S, C277S) was generated by site-directed mutagenesis PCR using pDONR223-p53-WT as a template using the primers indicated in Table S1. Plasmids (pcDNA3) expressing Flag-His-p53-WT and -cysteine mutant were obtained through Gateway cloning (Life Technologies) following the standard procedure.

Stable, doxycycline-inducible p53 expressing cells were generated by transduction with lentiviral pInducer20-Flag-p53 in the p53-KO RPE^{Tert} or H1299 background, followed by the selection with 400 μg/ml (for RPE^{Tert} cells) and 600 μg/ml (for H1299 cells) Neomycin for 2 weeks. pInducer20 plasmid was a gift from Stephen Elledge (Addgene plasmid # 44,012) [28]. pInducer20-Flag-p53 was made through Gateway cloning following standard procedures [29]. The inducible expression of p53 was confirmed by Western blotting and polyclonal cells were used for subsequent experiments.

2.4. Western blotting

RPE^{Tert} or H1299 cells were seeded in 6-well dishes and growing to be around 80% confluency, followed by treatments with different compounds for the indicated time. Cells were then directly scraped in 1× sample buffer (2% SDS, 5% 2-mercaptoethanol, 10% glycerol, Tris-HCl pH 6.8, 0.002% bromophenol blue). Samples were run on SDS-PAGE gels (Biorad system), followed by a standard Western blotting precure. Briefly, samples were transferred to polyvinylidene difluoride (PVDF) or nitrocellulose membranes. Membranes were then blocked with 2% BSA

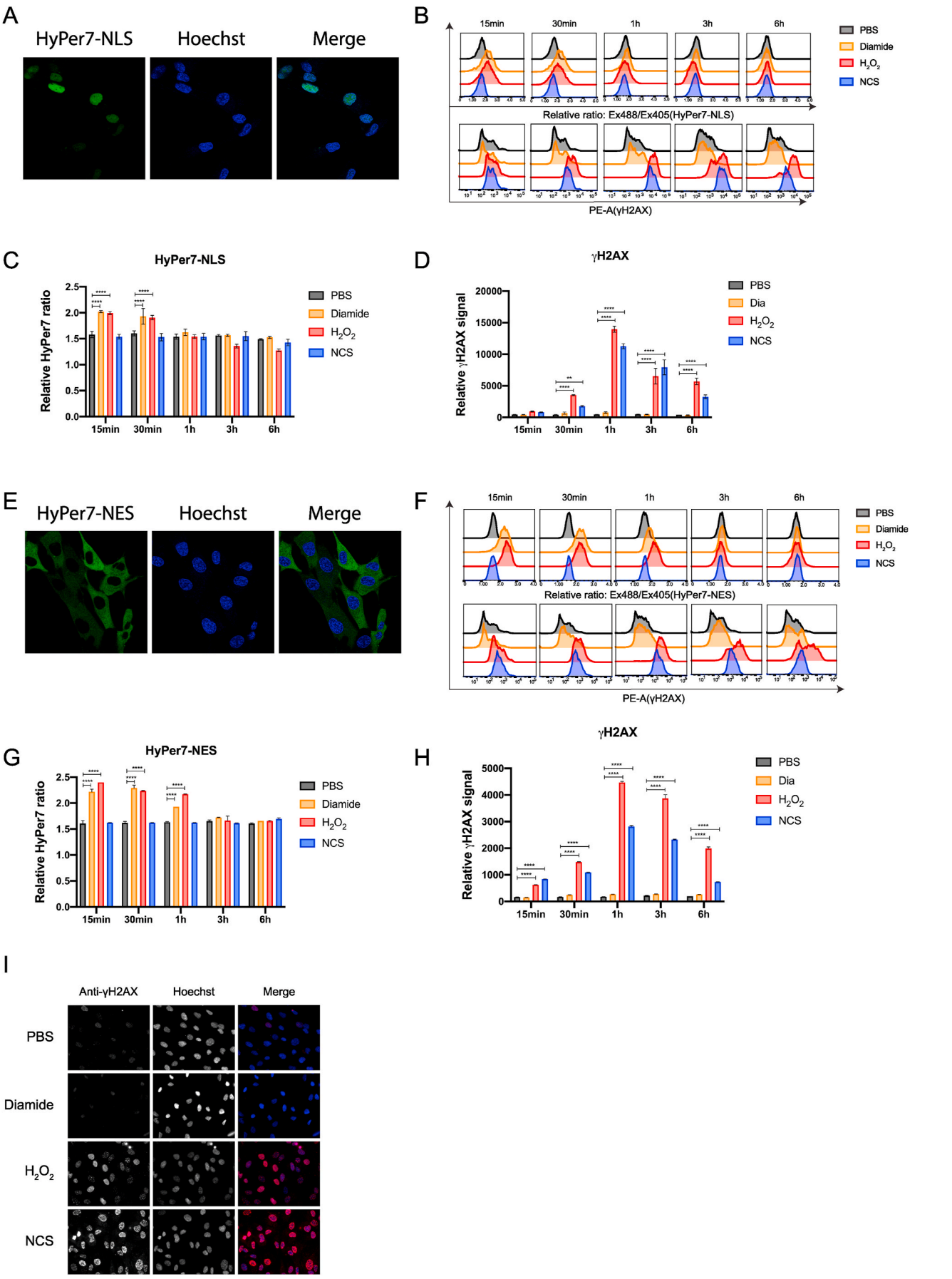

(caption on next page)

Fig. 1. Oxidative signaling and DNA damage signaling can be induced independent of each other
(A) Microscopy staining nuclear localized HyPer7(HyPer7- NLS) in RPE^{Tert} cells. Nuclei were stained with Hoechst.
(B) RPE^{Tert} cells stably expressing HyPer7- NLS were treated with PBS, diamide (200 μM), H_2O_2 (200 μM) or Neocarzinostatin (NCS) (250 ng/ml) for the indicated times. The relative ratio of oxidized (Ex 488 nm/Em 530/30 nm) over reduced (Ex405 nm/Em 525/50 nm) HyPer7 and the level of γH2AX (H2AX-pSer139) were evaluated by Flow Cytometry.
(C) Quantification of the relative HyPer7- NLS ratio (geometric mean of the histogram of the HyPer7 ratio distribution) from three independent experiments. The error bars stand for the standard deviation (SD) in these ratios. The statistical analysis was performed by using One-way ANOVA followed by Multiple comparisons test (Dunnett) for each time point. *, p value < 0.05; **, p value < 0.005, ***, p value < 0.0005, ****, p value < 0.0001.
(D) Quantification of the relative γH2AX signal (geometric mean of the histogram of the γH2AX signal distribution) from three independent experiments. The error bars stand for the standard deviation (SD) in these geometric means. The statistical analysis was performed by using One-way ANOVA followed by Multiple comparisons test (Dunnett) for each time point. *, p value < 0.05; **, p value < 0.005; ***, p value < 0.0005; ****, p value < 0.0001.
(E) Microscopy staining cytoplasmic localized HyPer7(HyPer7-NES) in RPE^{Tert} cells. Nuclei were stained with Hoechst.
(F) RPE^{Tert} cells stably expressing HyPer7- NES were treated with PBS, diamide (200 μM), H_2O_2 (200 μM) or Neocarzinostatin (NCS) (250 ng/ml) for the indicated times. The relative ratio of oxidized (Ex 488 nm/Em 530/30 nm) over reduced (Ex405 nm/Em 525/50 nm) HyPer7 and the level of γH2AX (H2AX-pSer139) were evaluated by Flow Cytometry.
(G) Quantification of the relative HyPer7- NES ratio (geometric mean of the histogram of the HyPer7 ratio distribution) from three independent experiments. The error bars stand for the standard deviation (SD) in these ratios. The statistical analysis was performed by using One-way ANOVA followed by Multiple comparisons test (Dunnett) for each time point.*, p value < 0.05; **, p value < 0.005, ***, p value < 0.0005, ****, p value < 0.0001.
(H) Quantification of the relative γH2AX signal (geometric mean of the histogram of the γH2AX signal distribution) from three independent experiments. The error bars stand for the standard deviation (SD) in these geometric means. The statistical analysis was performed by using One-way ANOVA followed by Multiple comparisons test (Dunnett) for each time point. *, p value < 0.05; **, p value < 0.005; ***, p value < 0.0005; ****, p value < 0.0001. Note that although the relative values are lower than in the HyPer7-NLS cell line, the dynamics of the induction are similar.
(I) Epifluorescence microscopy staining for γH2AX in RPE^{Tert} cells upon 1 h treatment of diamide (200 μM), H_2O_2 (200 μM) or NCS (250 ng/ml). Nuclei were stained with Hoechst and γH2AX were stained with an *anti*-γH2AX primary antibody and Alexa Fluor 568 as the secondary antibody.

TBS-Tween (TBST, 1% v/v) solution for 1 h at 4 °C, followed by incubation with primary antibodies overnight at 4 °C. After washing the membrane with TBST solution, secondary antibody staining was performed using HRP or fluorescence-conjugated antibodies for 1 h at 4 °C. After washed three times with TBST, membranes were analyzed by Image Quant LAS or Typhoon-Biomolecular Imager.

2.5. Ubiquitinylation assay

HEK293T cells were transiently transfected with Flag-His-p53 and His-ubiquitin expression constructs. After 48 h, cells were treated with or diamide (15 min) followed by lysis in buffer containing 100 mM NaH_2PO_4/Na_2HPO_4, 10 mM Tris pH 8, 8 M Urea, 10 mM Imidazole and 0.2% Triton X-100 and sonication. Cell lysates were then centrifuged at 10,000 rpm for 10 min, and 50 μl of supernatant was taken as input sample and ubiquitinated proteins were enriched by incubation with Ni-NTA beads for 2 h at room temperature. The Ni-NTA beads were washed twice with the above indicated lysis buffer, followed by a wash with elution buffer (100 mM NaCl, 20% glycerol, 20 mM Tris pH 8.0, 1 mM DTT and 10 mM Imidazole). In the end, ubiquitinated proteins were resuspended in 1× sample buffer (2% SDS, 5% 2-mercaptoethanol, 10% glycerol, Tris-HCI pH 6.8, 0.002% bromophenol blue), boiled at 95 °C for 8 min, and further analyzed by standard Western blotting.

2.6. Immunofluorescence microscopy

RPE^{Tert} cells were grown on glass coverslips in 6-well dishes for three days and then treated with PBS, diamide, or NCS for 1 h. Cells were washed twice with cold PBS and fixed (3.7% Formaldehyde solution) for 15 min at room temperature. Fixed cells were permeabilized using 0.1% Triton for 5 min followed by blocking with 2% BSA (w/v) plus purified goat IgG in 1:10,000 in PBS for 30–60 min at room temperature. After that, cells were incubated with primary antibodies (1:500 dilution for *Anti*-p53 and pH2AX (Ser139)) overnight, followed by 1 h incubation with secondary antibodies labeled with Alexa fluor 568 (ThermoFisher) and Hoechst 33,342 (Life Technologies) after washing twice with PBS. All antibody incubations were performed at 4 °C and in the dark. Coverslips were mounted with a drop of mounting medium, sealed with nail polish to prevent drying, and saved in the dark at 4 °C until analysis. Imaging was performed on a Zeiss Axio Imager Z1 and images were processed using ImageJ software.

HyPer 7-NLS and NES RPE^{Tert} were grown in 35 × 10 mm cellview cell culture dishes (627,860, Greiner). Live cells were stained with Hoechst 33,342 (Life Technologies) for 15 min at room temperature and imaged on a ZEISS confocal laser scanning microscope (LSM880).

2.7. RNA isolation and qPCR

Total RNA was isolated from Doxycycline-inducible p53 expressing RPE^{Tert} p53 KO cells (treated with or without doxycycline) using the RNeasy kit (QIAGEN). 500 ng RNA was used for cDNA synthesis using the iScript cDNA Synthesis Kit (BIO-RAD) according to the manufacturer's instructions. qPCR experiments were carried out using SYBR Green FastStart Master Mix [30] on a CFX Connect Real-time PCR detection system (Bio-RAD). qPCR cycle settings were as follows: pre-denaturation at 95 °C for 10 min, followed by 39 cycles of denaturation at 95 °C for 10 s, annealing at 58 °C for 10 s, and extension at 72 °C for 30 s. Relative gene expression was calculated using $2^{-\Delta\Delta CT}$ method by taking GAPDH as a reference gene. All the primers used for qPCRs are shown in Table S1.

2.8. Cell viability assay

Cell viability was evaluated using a dual Calcein-AM/Sytox-Blue assay, where Calcein-AM is used to stain live cells and Sytox blue to identify dead cells. 1×10^4 RPE^{Tert} and RPE^{Tert} p53 KO cells were seeded in 96-well plates. The next day, cells were treated with diamide, H_2O_2 or NCS at the indicated concentrations for 72 h, followed by addition of a mix of Calcein-AM/Sytox Blue at a final concentration of 1 μM for both dyes. The plates were mixed gently and incubated at 37 °C for 30 min, and then evaluated on a Spectra Max Fluorometer: Ex. 485 nm/Em 535 nm for Calcein and Ex. 444 nm/Em 460 nm for Sytox-Blue. The ratio of Calcein/Sytox-Blue was calculated and relative cell viability was determined by normalizing to untreated cells (considered as 100% cell viability).

2.9. Flow cytometry

To assess the effect of the various treatments on the DNA damage response and H_2O_2-dependent redox state (measured as the ratio of oxidation and reduction of the H_2O_2-specific sensor HyPer7), RPE^{Tert} cells stably expressing HyPer7-NLS and NES were treated with diamide, or NCS for the indicated times. To prevent post-harvest HyPer7 oxidation or reduction, cells were washed with PBS containing 100 mM NEM

prior to trypsinization. Cells were then fixed with 4% Formaldehyde solution for 10 min at room temperature, followed by incubation with ice-cold 70% Ethanol overnight at 4 °C. Cells were resuspended in PBS and washed with PBS buffer twice, and stained with *anti*-Phospho-Histone H2AX (Ser139) PE-conjugated antibody (0.25 μg/sample) for 30 min at room temperature. After that, cells were resuspended in PBS buffer with 1% BSA and 0.05% Tween and analyzed on a FACSCelesta Flow Cytometer (BD Bioscience). HyPer7 fluorescence was detected using Ex405/Em525/50 (reduced) and Ex488/Em30/30 (oxidized) lasers and filter sets.

For cell cycle profile assessment, dox-inducible p53 expressing RPE^{Tert} p53 KO cells with or without Dox addition were treated with H_2O_2, diamide or NCS. After 24 h, cells were washed with PBS, trypisinized, and fixed with 70% ethanol overnight at 4 °C. Cells were washed twice with and resuspended in staining buffer (PBS with 0.1% BSA and 0.05% Tween and DAPI) for 30 min in the dark on ice. Cells were then analyzed on a FACSCelesta Flow Cytometer (BD Bioscience).

Cell death was assessed using Propidium Iodide (PI) (sigma-Aldrich) exclusion and Annexin V-FITC (IQ Products) staining. RPE^{Tert} p53 KO cells and H1299 cells with or without doxycycline were treated with diamide, H_2O_2 or NCS for 24 h. Culture media, PBS buffer used to wash cells and trypsinized cells were collected in the same tube. Samples were washed once with PBS and resuspended in 1× Annexin V Binding Buffer (10 mM pH 7.4 HEPES, 140 mM NaCl and 2.5 mM $CaCI_2$) containing PI and Annexin V-FITC and incubated for 30 min in the dark on ice. Cells were then analyzed on a FACSCelesta Flow Cytometer (BD Bioscience).

2.10. Timelapse video fluorescence microscopy

Monoclonal RPE^{Tert} cells expressing either HyPer7-NLS or HyPer7-NES were plated in 8-well chamber slides (ibidi) and imaged using a Cell Observer microscope (Zeiss) with a 10× objective. The HyPer7 fluorescent protein was excited at 385 nm and 475 nm consecutively and the subsequent emission was measured using a BP514/44 filter. The different treatments were added after measuring the first timepoint, upon which imaging was continued.

Image processing was performed using FIJI imaging software. A background signal was obtained by imaging cells not expressing HyPer7, and this was subtracted from the HyPer7 images. The images were then thresholded to show only fluorescence inside cells and the images obtained with 495 nm excitation were divided by the images obtained by 385 nm excitation; This ratio describes the average degree of HyPer7 oxidation of all the cells in view (about 250 cells). Finally, the average ratio per timepoint was calculated per treatment and normalized to the first timepoint.

2.11. Statistical analysis

All statistical analysis was performed in GraphPad Prism 8 software. One-way ANOVA method followed by Dunnett's multiple comparisons, was used to evaluate the statistical significance of qPCR data, and an adjusted p value < 0.05 was considered to be statistically significant. A Student's t-test was used to evaluate the difference of cell death in p53-off and p53-on cells upon each treatment, and a p-value < 0.05 was considered to be statistically significant.

3. Results

3.1. Differential activation of oxidative signaling and the DNA damage response

H_2O_2 is known to induce signaling, part of which is mediated through the activation of stress-activated kinases (SAPK, e.g., JNK and p38 MAPK). But H_2O_2 also activates key kinases involved in the DNA Damage response (e.g., ATM and ATR) (Fig. S1A). Likewise, several genotoxic agents that are being used as chemotherapeutics have been suggested to act, at least in part, through the production of ROS and hence could start or modulate oxidative signaling and trigger stress-activated kinases (Fig. S1B-D).

To be able to dissect the DDR and oxidative signaling-based responses, we investigated whether it is possible to activate these pathways independently. To this end we stably expressed the H_2O_2-specific HyPer7 probe in non-transformed, human Telomerase immortalized Retinal Pigment Epithelial (RPE^{Tert}) cells using lentiviral transduction. RPE^{Tert} cells have been shown to have a wildtype p53 protein and response [31]. Some of the benefits of the HyPer7 probe as compared to earlier versions are its insensitivity to pH changes and enhanced sensitivity. The probe reports on the ratio of the H_2O_2 dependent oxidation (λ_{Ex}488 nm/λ_{Em} 530/30 nm) and reduction (λ_{Ex}405 nm/λ_{Em} 525/50 nm) by the thioredoxin system [24]. HyPer7 oxidation was assessed along with positivity for the DNA damage response marker H2AX-pSer139 (aka γH2AX) by flow cytometry upon treatment with diamide, H_2O_2 or Neocarzinostatin (NCS). In order to assess H_2O_2-dependent redox perturbations in the vicinity of the DNA, nuclear localized HyPer7 (HyPer7-NLS) was used (Fig. 1A). We found that it is indeed possible to induce the DDR and oxidizing conditions separately for prolonged time periods. The thiol-specific oxidant diamide, which is thought to act largely through oxidation of the GSH pool, rapidly but transiently induced HyPer7 oxidation, without affecting γH2AX levels for up to 6 h after treatment (Fig. 1B–1D, S2B, C). As mentioned, alterations in the ratio of the HyPer7 probe are a measure of the combined rate of oxidation (by H_2O_2) and reduction (by the thioredoxin system) [32], which makes it difficult to distinguish whether the diamide-induced increase in HyPer7 ratio stems from an increase of H_2O_2 from endogenous sources or from a loss of reductive power or both. In any case, the ratio of the H_2O_2-specific HyPer7 probe correlates with that of PRDX oxidation/reduction and hence is a good read-out for the induction of H_2O_2-dependent signaling. The DNA damaging agent NCS induced a buildup of γH2AX signal that peaked 1 h after treatment, without evidence of changes in the HyPer7 ratio. Treatment with H_2O_2 resulted in both HyPer7 oxidation and phosphorylation of H2AX, in line with the idea that this compound indeed induces both oxidative signaling and the DDR [33] (Fig. 1B-H, S2A, C). Note that the kinetics of H2AX phosphorylation by H_2O_2 follow those of NCS. The oxidation and reduction of HyPer7 upon diamide treatment occurs slightly slower as compared to H_2O_2. We next asked whether NCS could induce oxidative signaling in the cytoplasm, which has been proposed in a previous study [34]. To this end, we evaluated the HyPer7 ratio in RPE^{Tert} cells stably expressing cytoplasmic localized HyPer7 (HyPer7-NES) (Fig. 1E) as well as γH2AX positivity in parallel. Under the conditions used, NCS did not generate H_2O_2 in the cytoplasm either but again induced a substantial nuclear DNA damage response (Fig. 1F-H). Not surprisingly, both diamide and H_2O_2 treatment rapidly induced HyPer7 oxidation in the cytoplasm similar to what was observed for the nucleus (Fig. 1F, G). The induction of DNA damage by H_2O_2 and NCS but not by diamide in RPE^{Tert} cells was further corroborated by immunofluorescence microscopy (Fig. 1I), and over a broad range of concentrations by video timelapse fluorescence microscopy and Western blot (Fig. S2). H_2O_2 could be measured by the HyPer7 probe starting at a concentration of 5 μM bolus addition, and the signal was saturated above ~100 μM. DNA damage signaling was detected from concentrations as low as 25 μM (Fig. S1A, S2A, C). The induction of HyPer7 oxidation without evidence of DNA damage signaling by diamide was observed up until concentrations of ~250 μM. Above 500 μM, diamide did induce minor phosphorylation of CHK2 and H2AX (Fig. S2B, C) but also invariably led to complete loss of cell viability within 24 h irrespective of p53 status (see also Fig. S4). The dynamics of HyPer7 oxidation and reduction were slightly slower in case of diamide as compared to H_2O_2 (Fig. S2A, B). Taken together, diamide and NCS can serve as model compounds in this study to dissect to what extent the effects of H_2O_2 treatment are mediated through oxidative signaling, the DDR or both. Furthermore, these data already indicate that oxidizing conditions do not necessarily lead to

a DDR.

3.2. Oxidative signaling activates p53 independent of the DDR

Now that we had found means to selectively induce oxidizing conditions without triggering the DDR, we set out to explore whether and how this contributes to p53 stabilization and activation upon exposure to H_2O_2. To this end, RPE^{Tert} cells were exposed to diamide or H_2O_2 for various timepoints (Fig. 2A). NCS was used as a positive control for DDR activation in the absence of oxidative signaling (as shown in Fig. 1B). In line with the absence of γH2AX induction in the previous experiment, diamide also did not trigger the DDR pathway, as evidenced by the absence of ATM-pS1981, CHK2-pThr68, CHK1-pSer345 and p53-pSer15 induction. Nevertheless, prolonged (6 h) treatment with diamide surmounted in p53 stabilization to comparable levels as those induced by NCS (1 h) or H_2O_2 (6 h), and this was accompanied by accumulation of the p53 transcriptional target gene product p21 (Fig. 2A). Indeed, p21 was not induced in CRISPR/CAS9-derived RPE^{Tert} p53 KO cells (Fig. 2B). Both oxidizing compounds (but not NCS) trigger JNK (T183/Y185) phosphorylation, albeit more pronounced by diamide, indicating that the SAPK pathway acts downstream of oxidative signaling and independent of the DDR. Note that the stabilization of p53 by H_2O_2 and diamide was observed long after JNK or CHK2 phosphorylation had ceased.

To further elucidate signaling downstream of oxidative signaling and the DDR, we assessed whether ATM activity was required for the observed stabilization of p53 by oxidizing (diamide/H_2O_2) versus DNA damaging (H_2O_2/NCS) conditions using the ATM inhibitor KU55933 (ATMi). Inhibition of ATM abolished p53 phosphorylation on Ser15 and stabilization induced by H_2O_2 and NCS, whereas it had no effect on diamide-induced p53 stabilization (Fig. 2C). This suggests that whereas the DDR downstream of H_2O_2 proceeds through ATM, oxidative signaling does not. Phosphorylation of CHK2, but not CHK1, in response to H_2O_2 was indeed largely abolished upon treatment with ATMi, suggesting that ATM and not ATR signaling plays a dominant role in p53 activation upon H_2O_2-induced DNA damage (Fig. 2C). Diamide induced the activation of JNK and p38 MAPK to a larger extent as compared to H_2O_2, and this was also not affected by treatment with ATMi. If oxidative signaling-induced p53 stabilization depends on SAPK activation, this observation could be an explanation as to why oxidative signaling downstream of H_2O_2 fails to stabilize p53 in the presence of ATMi; something we will explore later in this study.

P53 has been reported to undergo cysteine oxidation upon oxidizing conditions (e.g., diamide treatment) both in vitro and in live cells [35]. To test whether cysteine oxidation plays a potential role in diamide and H_2O_2-mediated p53 stabilization, we devised a Flag-tagged p53 triple cysteine mutant (C182S, C229S, C277S), which was expressed from a doxycycline-inducible promoter in RPE^{Tert} p53 KO cells. The other cysteines in p53 are either not surface-exposed or are part of the Zn-finger and crucial for p53 structure (Fig. S3A) [36,37]. C182 and C277 were shown to be most sensitive to oxidation [35,38]. This triple cysteine mutant was still stabilized upon treatment with diamide or H_2O_2 (Fig. S3B), suggesting that redox modifications on these cysteines do not significantly contribute to p53 protein stabilization in response to oxidative signaling.

Collectively, our results indicate that oxidative signaling and the ATM-dependent DNA damage signaling responses as observed upon H_2O_2 exposure can be induced independent of each other, and that both pathways can lead to p53 stabilization and activation.

3.3. Diamide and H_2O_2 stabilize p53 through inhibition of its ubiquitin-dependent degradation

Several cellular stresses, including DNA damage, have been shown to induce stabilization of p53 through interference with MDM2-dependent ubiquitinylation and subsequent proteasomal degradation [39,40]. To explore whether diamide and H_2O_2-induced p53 stabilization also depend on inhibition of protein breakdown, p53 protein decay dynamics were assessed in the presence of these compounds in combination with the protein synthesis inhibitor cycloheximide (CHX). P53 levels rapidly declined under control conditions and persisted upon treatment with the positive control Nutlin-3a (an MDM2 inhibitor). Treatment with diamide, and to a lesser extent H_2O_2, resulted in attenuated p53 decay, suggesting that these oxidants interfere with MDM2-dependent degradation (Fig. 3A, B). In accordance, ubiquitinylation of p53 was inhibited upon diamide and H_2O_2 treatment (Fig. 3C). Several enzymes involved in the (de)ubiquitinylation reaction depend on catalytic cysteines and thus may be negatively regulated through oxidation. However, total protein ubiquitinylation appeared unaffected suggesting a specific effect of oxidants on ubiquitin-dependent p53 degradation (Fig. 3C).

3.4. Diamide and H_2O_2 dependent p53 activation are mediated by different stress activated protein kinases (SAPKs)

To further investigate how p53 was stabilized and activated by redox-dependent signaling, we made use of inhibitors of JNK and p38 MAPK kinases (Fig. 4A): two SAPKs that have previously been shown to be activated by oxidative signaling and that have both been implicated in p53 activation [5,6,41], Also in our experiments these pathways were activated by both diamide and H_2O_2, although diamide generally resulted in a slightly stronger activation (see also earlier in Fig. 2). Pre-treatment with the JNK inhibitor SP600125 almost completely abolished H_2O_2 induced p53 stabilization and activation, evidenced by loss of p21 induction, whereas diamide-dependent signaling towards p53 remained unaffected. Conversely, inhibition of p38 MAPK by pre-treatment with PH797804 largely blocked diamide-induced p53 stabilization and p21 induction, but did not inhibit H_2O_2 induced p53 stabilization. Note that the effect of PH797804 on p53 was evident despite some p38 MAPK activity remained as judged by the phosphorylation status of its target ATF2-pT71. (Fig. 4B). Pre-treatment with both inhibitors indeed blocked the induction of p53 and p21 induced by either oxidative signaling stimulus (Fig. 4C). These observations strongly indicate that even though diamide and H_2O_2 both activate p38 MAPK and JNK, diamide-dependent p53 activation is mediated by p38 MAPK, whereas H_2O_2 mediated p53 activation is mediated by JNK. We showed earlier (Fig. 2) that H_2O_2 also requires ATM signaling, whereas p38 MAPK does not. The experiments using the JNK inhibitor suggest that under these conditions, ATM signaling is still active (induction of CHK2-pT68, Fig. 4B), but not sufficient for p53 activation. Apparently both JNK and ATM activity are needed for full activation of p53 by H_2O_2 treatment.

The specificity of kinase inhibitors depends on the type of inhibitor and the used concentration. IC50 values are often determined in vitro and do not necessarily reflect concentrations needed in tissue culture systems. We examined whether the used concentrations cross-reacted with other signaling pathways downstream of H_2O_2. As is clear from Fig. 4A, SP600125 inhibited diamide and H_2O_2-induced JNK activation (pJNK and p-*c*-Jun), but did not greatly affect the phosphorylation of CHK1, CHK2, ERK and P38MAPK. Likewise, the p38 MAPK inhibitor PH797804 did not affect JNK, CHK1, CHK2 or ERK phosphorylation, and combined SP600125 and PH797804 inhibition did not affect CHK1, CHK2 or ERK phosphorylation (Fig. 4C, D). Although it is difficult to exclude any off-target effects altogether, these results indicate that at least the pathways under study are selectively inhibited by the used treatments.

3.5. Oxidative signaling activates p53-dependent transcriptional activity

The above presented data (Fig. 2 and 4) already show that activation of oxidative signaling either by diamide or H_2O_2 treatment induces p21 expression in a p53 dependent manner. The notion that DDR and oxidative signaling dependent p53 activation proceeds through different

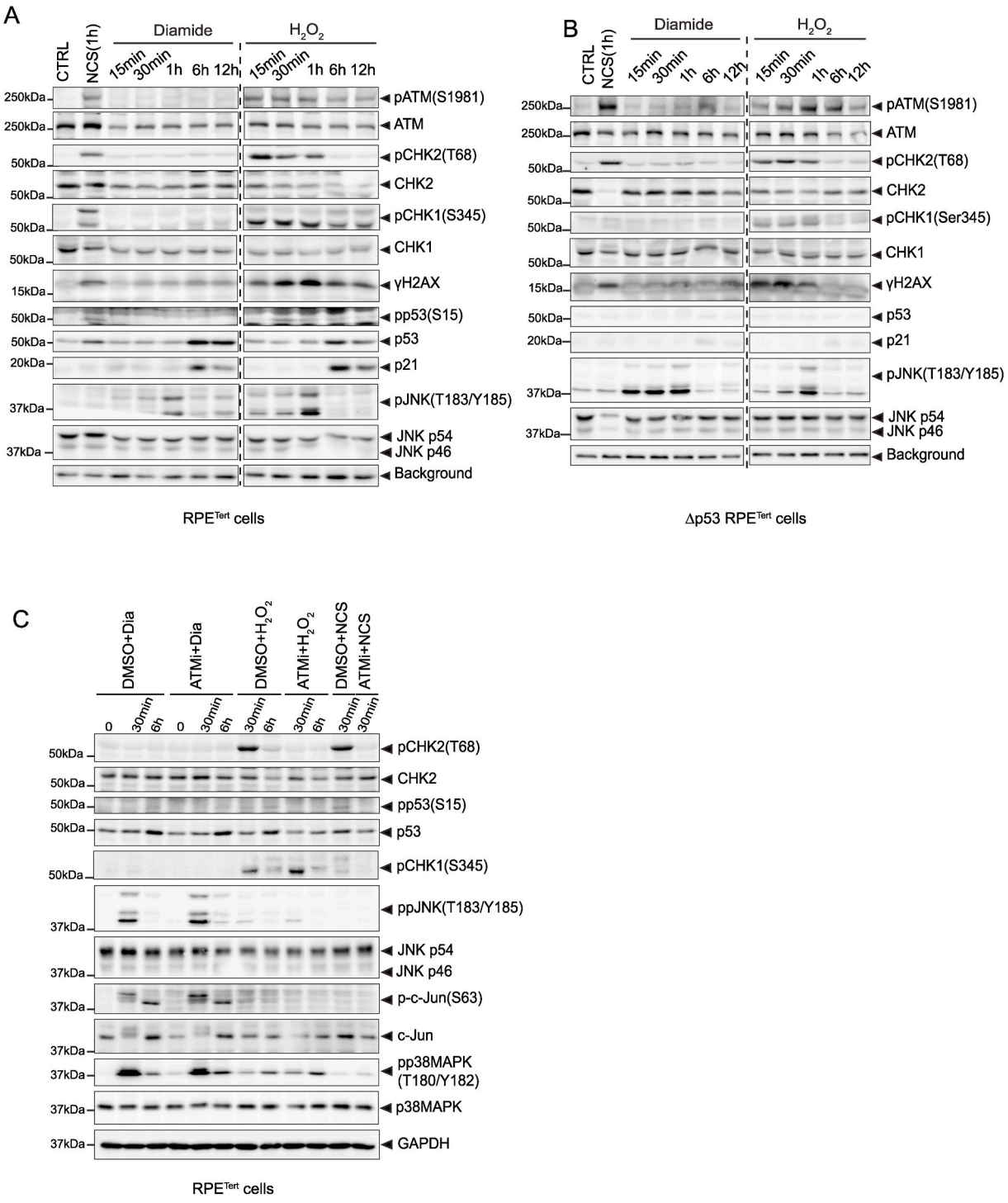

Fig. 2. Oxidative signaling activates p53 independent of the ATM-dependent DNA damage response

(A) RPE^{Tert} cells were treated with NCS (250 ng/ml), diamide (200 μM) and H_2O_2 (200 μM) for the indicated time. Phosphorylation states of ATM (S1981), CHK2 (T68), CHK1(S345), H2AX (S139), p53(S15), JNK (T183/Y185), endogenous p53 and p21 levels, and the total protein level of ATM, CHK2, CHK1 and JNK were evaluated by immunoblotting.

(B) Same treatment as in (A), but using RPE^{Tert} p53 KO cells.

(C) RPE^{Tert} cells were pretreated with DMSO or ATM inhibitor (ATMi) KU55933 (10 μM) for 1 h, followed by treatment with diamide (200 μM), H_2O_2 (200 μM) or NCS (250 ng/ml) for the indicated time. P53 level, phosphorylation state of CHK2(T68), CHK1(S345), p53(S15), JNK(T183/Y185), p38 MAPK(T180/Y182) and p-*c*-Jun (S63), and the total protein level of CHK2, JNK, *c*-Jun, p38 MAPK and GAPDH as a loading control were evaluated by immunoblotting.

All Western blots are representative of at least 3 replicate experiments.

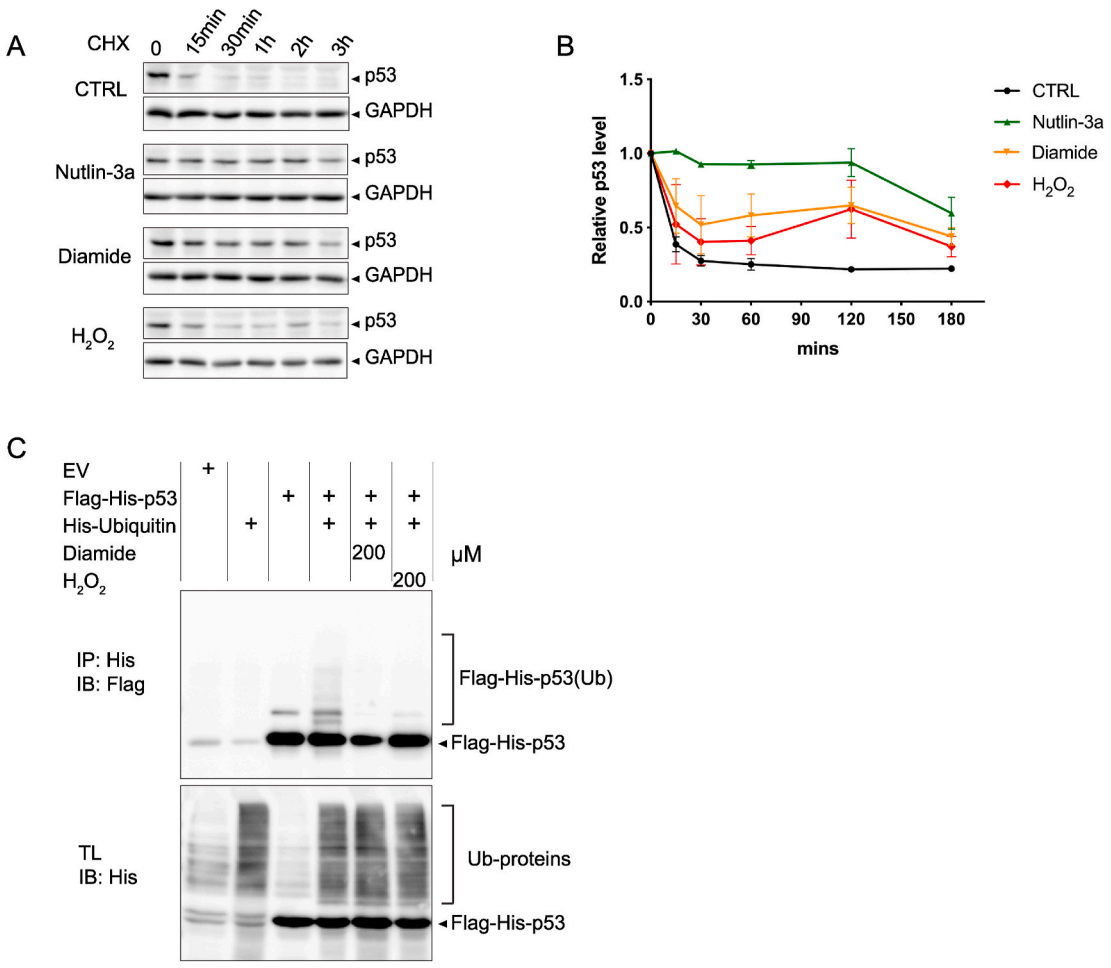

Fig. 3. Diamide and H_2O_2 stabilize p53 by inhibition of protein degradation and ubiquitinylation
(A) RPE^{Tert} cells were treated with Cycloheximide (CHX, 10 μg/ml) to block protein synthesis and at the same time exposed to Nutlin-3a (10 μM), diamide (200 μM) or H_2O_2 (200 μM) for the indicated time. Total cell lysates were loaded for evaluating the levels of endogenous p53 and GAPDH (as a loading control).
(B) Quantification of p53 protein intensity relative to GAPDH shown in (A) from two independent experiments.
(C) HEK293T cells expressing Flag-His-p53 alone or in combination with His-ubiquitin were treated with diamide (200 μM) or H_2O_2 (200 μM) for 15 min P53 ubiquitinylation was evaluated by His-pulldown using Ni-NTA beads and immunoblotting with anti-Flag antibody. The presented data are representative for three independent experiments.

upstream kinase signaling cascades could in principle lead to an induction of different p53 transcriptional targets due to alternative PTM or cofactor binding. In order to evaluate p53-dependent gene transcription we established doxycycline-inducible Flag-p53 expressing RPE^{Tert} p53 KO cells. Doxycycline (dox) treatment was optimized to induce Flag-p53 levels similar to endogenous p53 in the parental RPE^{Tert} cell line under basal conditions (4 ng/ml dox treatment for 48 h or 72 h, Fig. 5A). Ectopically expressed Flag-p53 in these cells mimicked the response to diamide and H_2O_2 observed in wildtype RPE^{Tert} cells (Fig. 5B). Next, we evaluated the expression of *TP53* itself and some of its target genes associated with cell cycle arrest (*CDKN1A* and *GADD45a*), apoptosis (*BAX* and *PIG3*), p53 turnover (*MDM2*) and metabolism (*TIGAR*) upon oxidative signaling and DNA damage. We found that *TP53* mRNA levels were increased by almost 2-fold upon addition of doxycycline, and this was significantly increased by H_2O_2 treatment, suggesting that H_2O_2 regulates p53 levels not only at the level of stabilization (Fig. 5C, 4A, B). P53 transcriptional targets *CDKN1A* (p21), *GADD45a* and *PIG3* were further activated both by oxidative signaling and DDR signaling to p53 to some extent, whereas *MDM2 and BAX* were significantly induced only by DNA damage signaling to p53 (H_2O_2 and NCS) (Fig. 5C). No obvious change in the induction of *TIGAR* was observed upon either treatment. Collectively, these observations suggest that both oxidative signaling and the DDR can activate p53, and that there seems to be some target selectivity depending on which upstream pathway activates p53.

3.6. *Oxidative signaling and DNA damage trigger p53-dependent cell cycle arrest and cell death*

To further examine the biological consequences of p53 activation by oxidative signaling and DNA damage, we evaluated cell viability in RPE^{Tert} and RPE^{Tert} p53 KO cells in response to addition of diamide, H_2O_2 and NCS (Fig. S4). Especially diamide and H_2O_2 treatment resulted in a higher loss of cell viability in a p53-dependent manner. To better understand the cause of the reduced cell viability when p53 was present, we assessed cell cycle profiles in RPE^{Tert} p53 KO cells expressing doxycycline inducible p53 upon diamide, H_2O_2 and NCS treatment for 24 h. We observed that both oxidative signaling and DNA damage triggers a mild p53-dependent cell cycle arrest with cells ending up with 4 N DNA (Fig. 6A, B), meaning that they are likely arrested in G2 or M phase or arrest in G1 upon mitotic bypass after replication [42]. Furthermore, we observed that both diamide and H_2O_2 treatment induced significantly more cell death following p53 expression, indicating that oxidative signaling can trigger p53-dependent cell death (Fig. 6C, D). Note that NCS did not induce pronounced cell death in RPE cells when p53 was inducibly expressed, whereas it did induce cell death in H1299 cells (Fig. S5A, B), which could be in line with the general notion that cancer

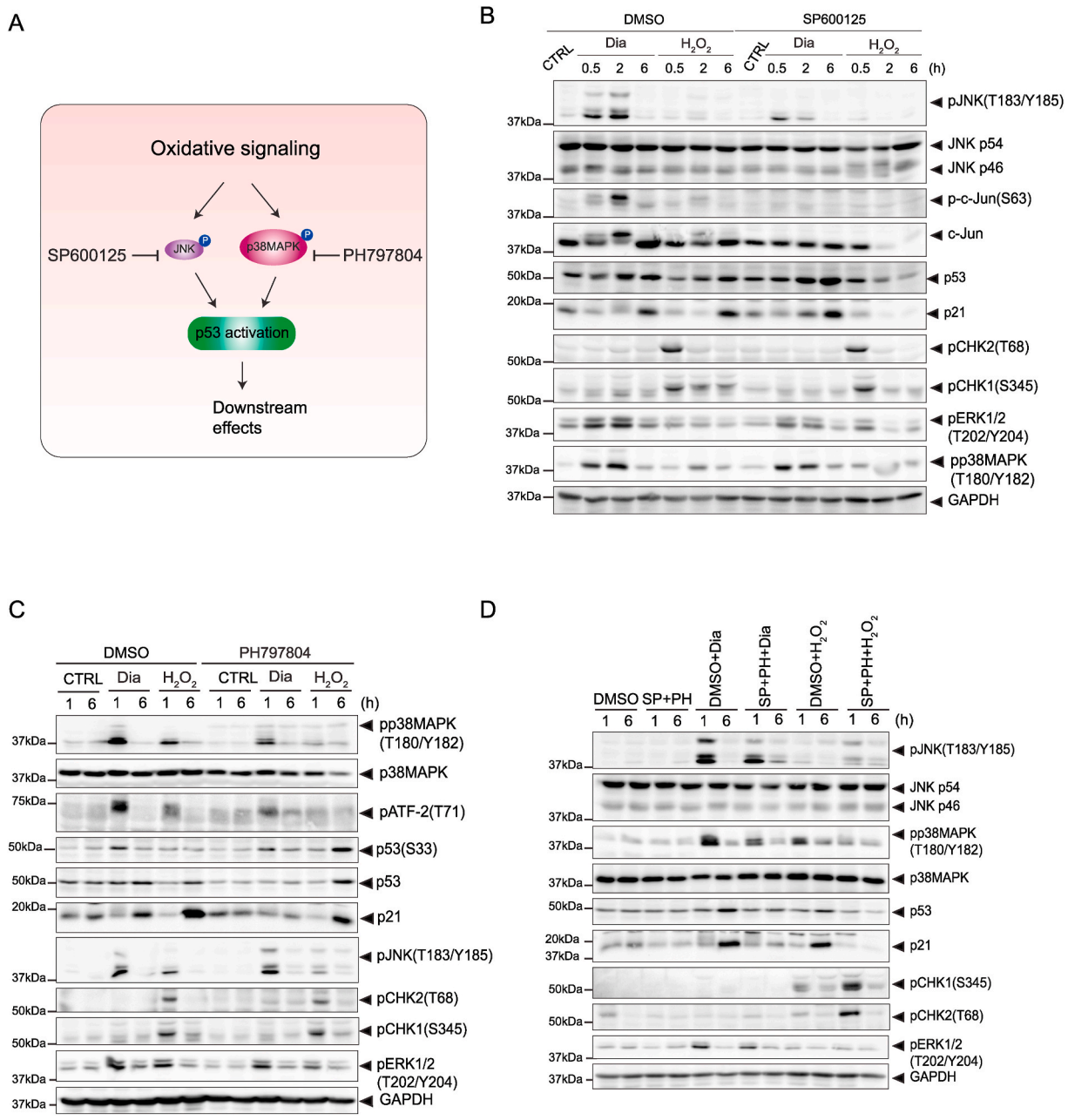

Fig. 4. P38 MAPK, not JNK, is required for oxidative signaling-mediated p53 activation.
(A) Overview of p53 activation through p38 MAPK
and JNK under oxidative signaling. P38 MAPK and JNK are activated in response to oxidative signaling, which leads to p53 activation. SP600125 and PH797804 are inhibitors for JNK and p38 MAPK, respectively.
(B) JNK is dispensable for diamide-mediated p53 activation, but is essential for H_2O_2-induced p53 activation. RPE^{Tert} cells were pre-treated with DMSO or SP600125 (20 μM) for 2 h, followed by treatment with diamide (200 μM) or H_2O_2 (200 μM) for the indicated time. The total protein levels of JNK (p54 and p46), *c*-Jun, p53, p21 and GAPDH, and phosphorylation states of JNK(T183/Y185), *c*-Jun (S63), CHK2(T68), CHK1(S345), ERK1/2 (T202/Y204) and p38 MAPK(T180/Y182) were detected by immunoblotting.
(C) p38 MAPK is indispensable for diamide-induced, but not for H_2O_2-induced p53 activation. RPE^{Tert} cells were pre-treated with DMSO or PH797804 (10 μM) for 2 h, followed by treatment with diamide (200 μM) or H_2O_2 (200 μM) for the indicated time. The total protein levels of p38 MAPK, p53, p21 and GAPDH, and phosphorylation states of p38 MAPK(T180/Y182), ATF-2 (T71), JNK(T183/Y185), CHK2(T68), CHK1(S345) and ERK1/2 (T202/Y204) were evaluated by immunoblotting.
(D) RPE^{Tert} cells were pre-treated with DMSO or SP600125 (20 μM) and PH797804 (10 μM) together for 2 h, followed by treatment with diamide (200 μM) or H_2O_2 (200 μM) for the indicated time. The total protein levels of JNK (p54 and p46), p38 MAPK, p53, p21 and GAPDH, and phosphorylation states of JNK(T183/Y185), p38 MAPK(T180/Y182), CHK2(T68), CHK1(S345) and ERK1/2 (T202/Y204) were evaluated by immunoblotting analysis.
All Western blots are representative of at least 3 replicate experiments.

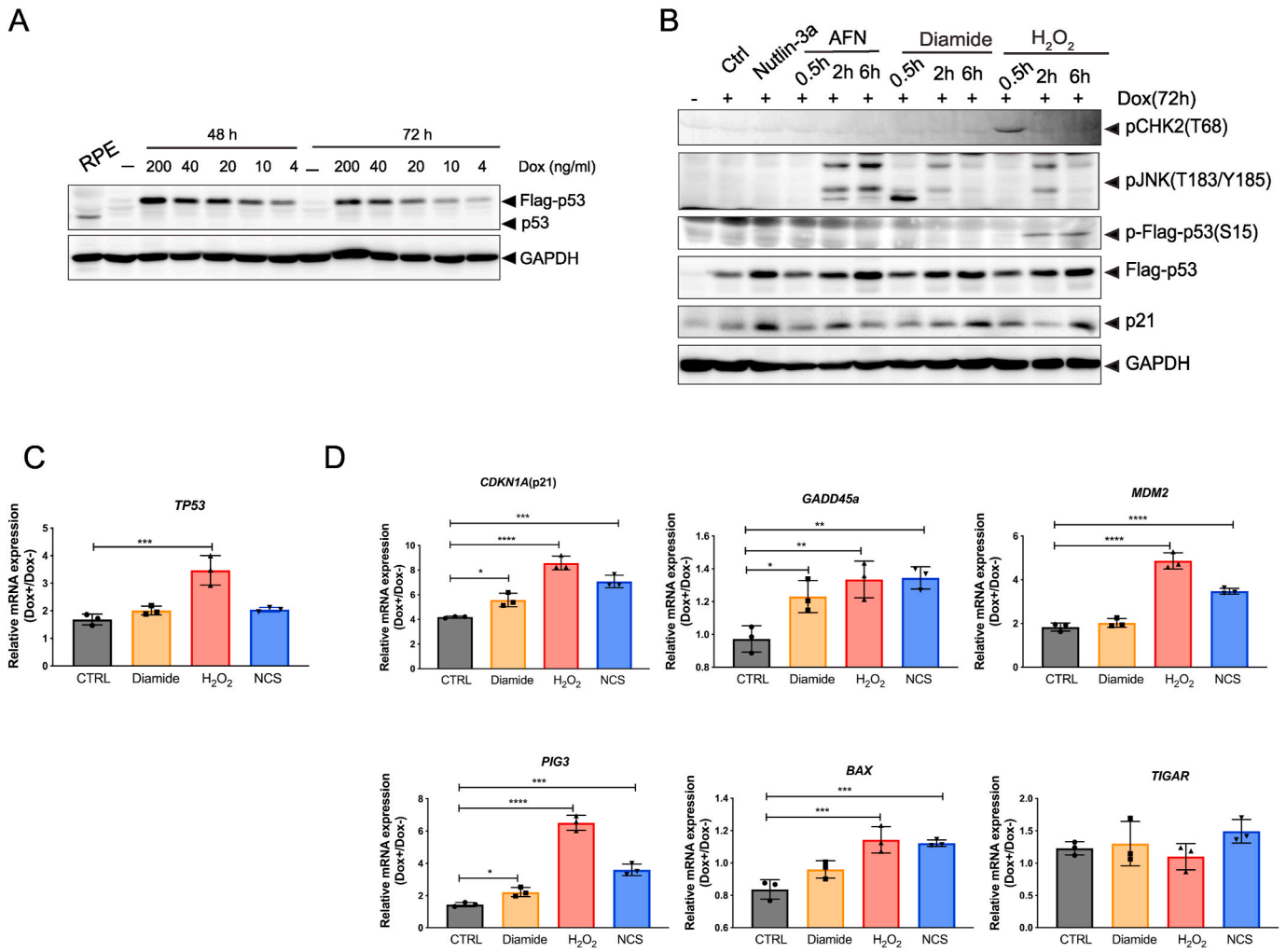

Fig. 5. Oxidative signaling induces p53-dependent transcriptional activation

(A) Immunoblotting analysis of RPE^{Tert} p53 KO cells expressing Dox-inducible p53, treated with a range of doxycycline (dox, 4–200 ng/ml). Wildtype p53 in RPE^{Tert} cells is used as a reference for endogenous levels.

(B) p53 expression was induced with 4 ng/ml Dox for 72 h to mimic near-endogenous levels, followed by treatment with Nutlin-3a (10 μM), Auranofin (AFN) (10 μM), diamide (200 μM) or H_2O_2 (200 μM) for the indicated time. Total cell lysates were analyzed for the levels of Flag-p53, p21 and GAPDH, and phosphorylation states of CHK2(T68), JNK(T183/Y182) and Flag-p53(S15) by immunoblotting.

(C) p53 expression was induced with 4 ng/ml Dox for 48 h, followed by treatment with diamide (200 μM), H_2O_2 (200 μM) or NCS (500 ng/ml) for 24 h. The expression of p53 target genes was measured in both Dox- (p53-off) and Dox+ (p53-on) cells by qPCR. The ratio of the gene expression (relative to GAPDH) in p53-on cells over that in p53-off cells was calculated to assess p53-dependent transcriptional target activation. The data is presented as the mean and standard deviation (SD) from three independent experiments. Statistical analysis was performed by using One-way ANOVA followed by Multiple comparisons test (Dunnett). *, p value < 0.05; **, p value < 0.005; ***, p value < 0.0005; ****p value < 0.0001.

cells are more vulnerable to chemotherapeutic drugs than untransformed cells [43]. Both diamide and H_2O_2 also induced p53-dependent cell death in H1299 cells (Fig. S5A, B). Collectively, our data reveal that oxidative signaling can activate p53 to induce cell death in the absence of the DDR both in untransformed and human cancer cells.

4. Discussion

The observations that exposure to ROS (H_2O_2, $O_2^{\bullet-}$, $HO^{\bullet}$) either from endogenous or exogenous sources can activate the DDR as well as p53 [4,14,44] has given credence to the idea that ROS activates p53 downstream of signaling in response to oxidative DNA damage. In line with this notion, (enhanced) mitochondrial respiration and the ensuing $O_2^{\bullet-}/H_2O_2$ production is frequently cited as a source of oxidative DNA damage and mutation in genomic DNA in tumors [17,18]. But H_2O_2 also acts as a second messenger in redox signaling, which plays an essential role in regulating protein functions and biological processes [12], including several phosphorylation cascades upstream of p53 [19,20]. In this paper we have used the term 'oxidative signaling' to discriminate DNA damage signaling and other signaling downstream of oxidants, because the term 'redox signaling' usually refers to endogenous oxidant levels rather than challenges with oxidants as a model for therapeutic treatments. The engagement of multiple signaling cascades downstream of oxidants has made it difficult to attribute p53 activation in response to elevated H_2O_2 levels to activation of the DDR, oxidative signaling or both [10]. What further complexes understanding ROS-induced p53 activation is the observation that ATM can also be activated by oxidative signaling in the absence of DNA damage [45]. Furthermore, treatment with several DNA damaging chemotherapeutic drugs, such as doxorubicin, cisplatin and 5-fluorouracil, can lead to enhanced ROS production (Fig. S1) [46,47]. In this work, we set out to dissect DNA damage signaling and oxidative signaling upstream of p53, by applying treatments that we titrated and validated to either induce only the DDR (as judged by gamma-H2AX, pCHK2 and CHK1), only oxidative signaling

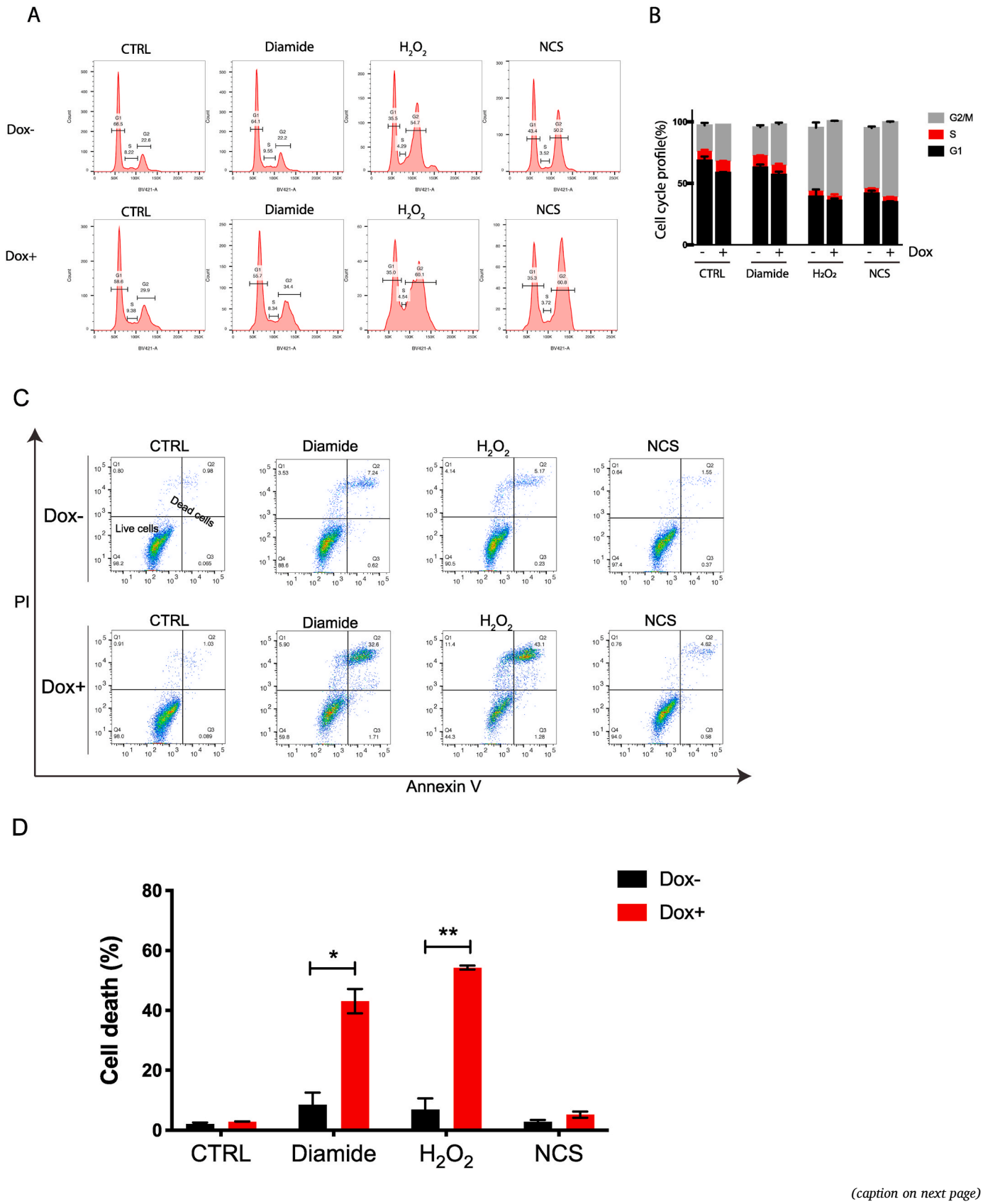

(caption on next page)

Fig. 6. Oxidative signaling and DNA damage induce p53-dependent cell cycle arrest and cell death
(A) Histogram plots showing cell cycle profile in Dox inducible expressing p53 RPE^{Tert} cells upon induction of redox and DNA damage signaling as measured by Flow Cytometry (DAPI staining). Dox-inducible expressing p53 RPE^{Tert} cells were cultured with or without Dox for 48 h, followed by the addition of diamide (200 μM), H_2O_2 (200 μM) and NCS (500 ng/ml) for 24 h. Cell cycle profile was then measured by Flow Cytometry using DAPI staining. The plots show representative samples from three independent experiments.
(B) Quantification of cell cycle profile from three independent experiments.
(C) Dot plots showing cell death in Dox inducible expressing p53 RPE^{Tert} cells upon induction of oxidative and DNA damage signaling as measured by Flow Cytometry (PI-exclusion assay). Dox-inducible expressing p53 RPE^{Tert} cells were cultured with or without Dox for 48 h, followed by the addition of diamide (250 μM), H_2O_2 (300 μM) and NCS (500 ng/ml) for 24 h. Cell death was then measured by Flow Cytometry using Propidium iodide (PI) staining. The plots show representative samples from three independent experiments.
(D) Quantification of cell death from three independent experiments. A student's t-test was used to analyse statistical difference in cell death between Dox- and Dox + RPE^{Tert} cells upon each treatment. *, p value < 0.05. **, p value < 0.005.

(as judged by oxidation of the H_2O_2 specific HyPer7 probe and SAPK activation) or both. NCS induced a DNA damage response, without evidence of elevated H_2O_2 within 6 h. Diamide only led to oxidative signaling without activation of the DDR, whereas H_2O_2 indeed induced both DDR and oxidative signaling, each with similar kinetics as observed for NCS and diamide respectively.

Other studies did find that treatment with NCS resulted in the elevated oxidation of 2,7-dichlorodihydrofluorescein ($DCFH_2$-DA) in U2OS cells [34]. The different cell lines used, specificity of the used detection method or drug concentrations applied may underlie this apparent discrepancy. Besides the lack of HyPer7 oxidation induced by NCS, we also found no evidence of NCS-induced oxidative signaling as judged by p38 MAPK or JNK activation in H1299 and HEK293T cells (not shown) at the concentration range used in this study, which we think further validates the approach. As mentioned, it has been shown that ATM can also be activated in the absence of DNA damage through disulfide-dependent homodimerization in response to oxidant treatment [21]. In contrast to our findings, that study found that both H_2O_2 and diamide were capable of disulfide-dependent activating ATM and subsequent p53-Ser15 phosphorylation, whereas we found no evidence that diamide could activate ATM as judged by p53-pSer15, CHK2-Thr68 or γ-H2AX in all cell lines we tested. On the other hand, the same study found induction of pCHK2 but not γ-H2AX in response to H_2O_2, whereas in our study H_2O_2 did induce both pCHK2 and γ-H2AX as well as activation of p38 MAPK and JNK, suggesting that H_2O_2 triggers both the canonical DDR along with oxidative signaling. Again, differences in the precise protocol for treatment and cell lines used might underlie these contrasting observations.

With the described selection of treatments that trigger only the DDR, only oxidative signaling or both we were able to dissect how p53 is activated upstream by these pathways. We observed that p53 was activated by DNA damage and oxidative signaling through distinct upstream kinases, that both seem to converge on the inhibition of MDM2-dependent p53 degradation (Fig. 7). It is not clear as yet whether this

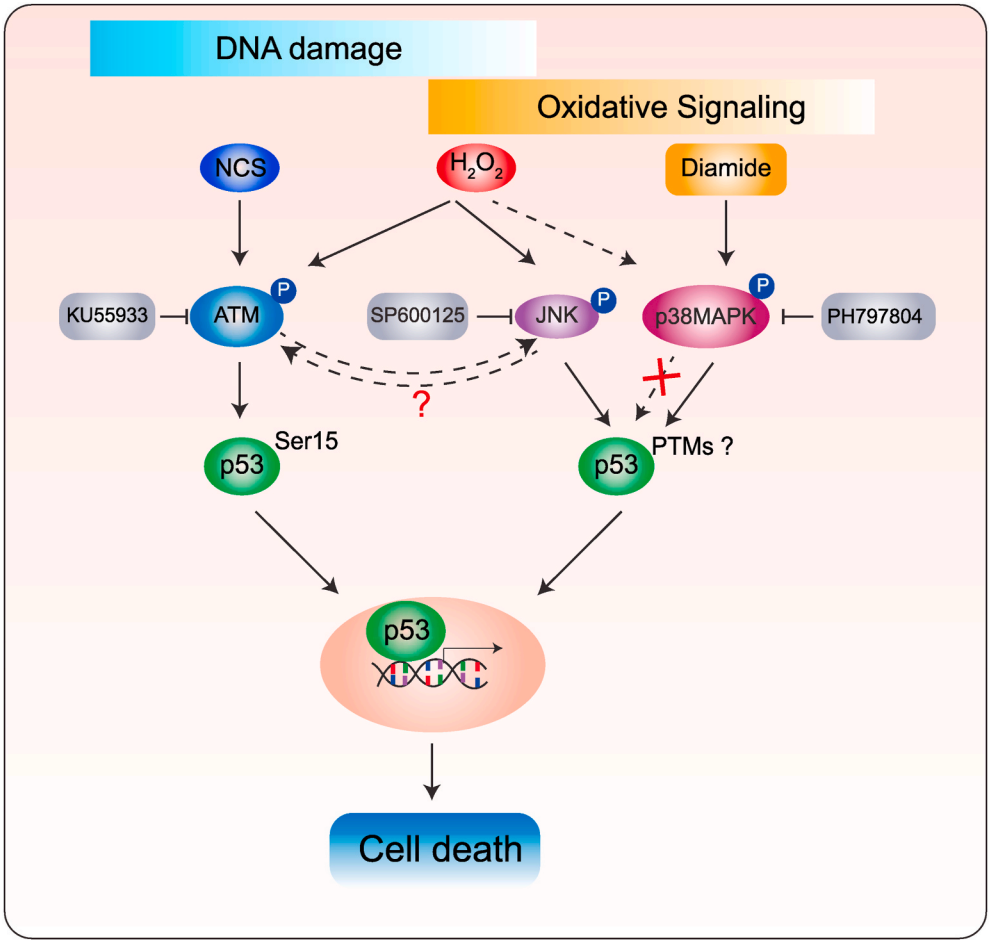

Fig. 7. Distinct upstream kinase-dependent signaling pathways activate p53 in response to DNA damage and oxidative signaling.
NCS and H_2O_2 both trigger the ATM-dependent DNA damage response and downstream p53 activation. Inhibition of ATM indeed abolishes NCS and H_2O_2-induced p53 activation. H_2O_2 also activates JNK, and this was also required for H_2O_2-induced p53 activation, whereas inhibition of JNK abrogated p53 activation by H_2O_2, no effects on the ATM pathway were observed, suggesting that JNK and ATM somehow mediate p53 activation through synergetic pathways, but the details remain to be unraveled. P38 MAPK is also activated by H_2O_2, but it was required for H_2O_2-induced p53 activation (dashed line). In contrast, diamide-induced oxidative signaling activates p53 through p38 MAPK, independent of ATM and JNK. p53 induces transcriptional target genes and cell death in response to both the DDR and oxidative signaling. Our data indicate that p53 can be activated by oxidative signaling without inducing collateral DNA damage, thereby lowering the risk for the acquisition of new mutations driving tumor progression and initiation.

is due to lower MDM2 levels or activity in response to oxidant treatment or loss of the p53-MDM2 interaction. In any case, protein (de)ubiquitinylation in general seemed unaffected by oxidant treatment (Fig. 3). ATM was required for p53 activation in response to NCS and H_2O_2-induced DNA damage, but dispensable for p53 activation induced by diamide-mediated oxidative signaling. P38 MAPK activity on the other hand was required for p53 stabilization and activation upon diamide-induced oxidative signaling, but not for NCS and H_2O_2-induced p53 activation. Our results furthermore showed that JNK was required for p53 activation by H_2O_2, although inhibition of ATM also completely blocked H_2O_2-induced p53 activation. This could suggest that ATM activation also somehow requires JNK activity in case of H_2O_2 dependent activation, although this remains to be further explored. H_2O_2 activates both JNK and p38 MAPK, which suggests that H_2O_2 treatment would still result in p53 stabilization in the presence of JNK inhibitor through the p38 MAPK pathway, but we did not find clear evidence for this. This could be because the extent of p38 MAPK activation by H_2O_2 is much lower as compared to diamide dependent activation, or there might be other undiscovered pathways induced by diamide but not H_2O_2 that act in concert with p38 MAPK.

ATM, p38 MAPK, JNK and p53 have all been shown to be subject to oxidative modification on cysteines [21,35,48,49]. Our data suggests that at least modification of surface-exposed, non-Zn-finger cysteines in p53 does not underlie p53 stabilization in response to oxidant treatment (Fig. S3). It will be interesting to explore whether differential cysteine oxidation of ATM, p38 MAPK and JNK in response to diamide versus H_2O_2 could explain the observed differential responses to these compounds.

We found that activation of p53 by both oxidative signaling and the DDR resulted in transcriptional activation of p53 targets, and there seemed to be some differential effects dependent on which pathways were activated. It has been proposed that different stresses, including oxidative signaling and DNA damage would lead to distinct transcriptional programs of p53 [50]. Differential regulation in response to specific stressors could stem from alternative co-factor binding, specific PTMs or the simultaneous engagement of parallel signaling pathways, and it has also been suggested that oxidant-induced p53 target gene promoters bear distinct p53 consensus motifs [51]. However, in our study we did not observe a black and white effect of p53-dependent gene expression in response to differential stresses. We found that p21, *GADD45a* and *PIG3* were induced by both oxidative signaling and DNA damage, whereas *MDM2* and *BAX* were more induced by DNA damage signaling upstream of p53 (H_2O_2 and NCS) than oxidative signaling (diamide). Since most previous studies did not carefully compare the induction of target genes in response to compounds that only induce the DDR or oxidative signaling, it is difficult to compare our observations to these studies. Furthermore, our selection of p53 target genes is rather limited and mostly aimed at showing that both DDR and oxidative signaling induced p53 stabilization also activates its transcriptional activity.

Arguably the prime p53-dependent tumor suppressive response is the induction of apoptosis, which is the goal of many anti-cancer therapies that are aimed at the reactivation or restoration of wild-type p53 function. Primary cancer-therapies including several chemotherapeutics and irradiation elicit DNA damage and trigger the DDR and downstream p53-dependent apoptosis in multiple tumor types [52,53]. Some chemotherapeutics used in the clinic, like Cisplatin and Doxorubicin have been shown to activate both JNK and p38 MAPK along with the DDR [7,54], but it is not entirely clear which of these pathways represents the dominant mechanism behind their efficacy. But the induction of DNA damage comes with the risk of generating new mutations. These may induce novel oncogenic events in surrounding tissue, but also drive tumor progression and therapy resistance through tumor evolution by mutation and selection. The data presented here suggest that p53 can be activated to trigger an apoptotic response independent of the DDR through oxidative signaling without risking the induction of collateral DNA damage and the ensuing tumor cell evolution. Several compounds have been developed with the aim to directly restore a p53 tumor suppressive response. Nutlin-3a and analogs for instance act by inhibition of MDM2 dependent ubiquitinylation of p53 and clinical trials using these compounds are underway [55] Another p53-directed compound, APR-246, that aims to refold mutant p53 was shown to bind directly to cysteines on p53, but also to other cellular thiols and thereby affect the cellular redox state, and it has been suggested that its effect could be due to a combination of these two [56], which could be in line with the findings described in this study.

Tumor cells, as compared to healthy cells, in general have higher ROS levels, for instance through altered metabolism, and as a result need to augment their antioxidant capacity in order to survive and thrive. It has been suggested that due to the simultaneously elevated production and scavenging of ROS in tumor cells, the redox state would be more easily tilted to more oxidizing [57]. With that in mind, further enhancing ROS levels using pro-oxidant approaches have been suggested as a strategy to induce tumor cell death [58]. But inhibition of the cellular reductive capacity, like we do here by using diamide, could in principle trigger a p53 response without the risk of collateral DNA damage as explained above. Such therapies may for instance be aimed at inhibition of the TrxR/Trx system (using e.g. Auranofin) [59,60] or depletion of NADPH [61] but it remains to be explored whether such approaches would indeed be feasible. Importantly, it will need to be established whether the here described p38 MAPK-dependent response to oxidants is functional in various wild-type p53 expressing cancer cell lines and tumor model systems. If so, the observation that oxidative signaling and the DDR activate p53-apoptosis through distinct upstream signaling cascades may contribute to new ideas for developing therapeutic strategies.

Author contributions

T.S. and T.B.D. designed the study and wrote the manuscript. B.M.T.B. reviewed and commented on the manuscript. T.S. performed most of the experiments. P.E.P established the doxycycline-inducible Flag-p53 expressing system in cells and assisted with experiments and laboratory management. D.M.K.v.S. cloned and produced HyPer7 lentivirus and performed video timelapse microscopy experiments.

Declaration of interests

The authors declare there is no conflict of interest.

Acknowledgments

We are grateful for suggestions and input from our colleagues at the department of Molecular Cancer Research, University Medical Center Utrecht. We thank Jeroen van den Berg and René Medema for sharing their RPE^{Tert} p53 KO cell line, and Vsevolod Belousov for sharing the HyPer7 construct. The work was made possible with grants from the China Scholarship Council (CSC no. 201606300046) to T.S. and from the Dutch Cancer Society (KWF UU 2014–6902) to T.B.D. B.M.T.B is part of the Oncode Institute, which is partly financed by the Dutch Cancer Society (KWF Kankerbestrijding) and was funded by the gravitation program CancerGenomiCs.nl from the Netherlands Organization for Scientific Research (NWO).

Appendix A. Supplementary data

Supplementary data to this article can be found online at https://doi.org/10.1016/j.freeradbiomed.2021.06.013.

References

[1] F. Kruiswijk, C.F. Labuschagne, K.H. Vousden, p53 in survival, death and metabolic health: a lifeguard with a licence to kill, Nat. Rev. Mol. Cell Biol. 16 (7) (2015) 393–405.
[2] A. Hirao, et al., DNA damage-induced activation of p53 by the checkpoint kinase Chk2, Science 287 (5459) (2000) 1824–1827.
[3] C.E. Canman, et al., Activation of the ATM kinase by ionizing radiation and phosphorylation of p53, Science 281 (5383) (1998) 1677–1679.
[4] N.H. Chehab, et al., Phosphorylation of Ser-20 mediates stabilization of human p53 in response to DNA damage, Proc. Natl. Acad. Sci. U. S. A. 96 (24) (1999) 13777–13782.
[5] D.V. Bulavin, et al., Phosphorylation of human p53 by p38 kinase coordinates N-terminal phosphorylation and apoptosis in response to UV radiation, EMBO J. 18 (23) (1999) 6845–6854.
[6] D.M. Milne, et al., p53 is phosphorylated in vitro and in vivo by an ultraviolet radiation-induced protein kinase characteristic of the c-Jun kinase, JNK1, J. Biol. Chem. 270 (10) (1995) 5511–5518.
[7] R. Sanchez-Prieto, et al., A role for the p38 mitogen-acitvated protein kinase pathway in the transcriptional activation of p53 on genotoxic stress by chemotherapeutic agents, Canc. Res. 60 (9) (2000) 2464–2472.
[8] Q.B. She, W.Y. Ma, Z. Dong, Role of MAP kinases in UVB-induced phosphorylation of p53 at serine 20, Oncogene 21 (10) (2002) 1580–1589.
[9] T. Buschmann, et al., Jun NH2-terminal kinase phosphorylation of p53 on Thr-81 is important for p53 stabilization and transcriptional activities in response to stress, Mol. Cell Biol. 21 (8) (2001) 2743–2754.
[10] T. Shi, T.B. Dansen, Reactive oxygen species induced p53 activation: DNA damage, redox signaling, or both? Antioxidants Redox Signal. 33 (12) (2020) 839–859.
[11] G.S. Wu, The functional interactions between the p53 and MAPK signaling pathways, Canc. Biol. Ther. 3 (2) (2004) 156–161.
[12] H. Sies, D.P. Jones, Reactive oxygen species (ROS) as pleiotropic physiological signalling agents, Nat. Rev. Mol. Cell Biol. 21 (7) (2020) 363–383.
[13] K.M. Holmstrom, T. Finkel, Cellular mechanisms and physiological consequences of redox-dependent signalling, Nat. Rev. Mol. Cell Biol. 15 (6) (2014) 411–421.
[14] L. Benitez-Bribiesca, P. Sanchez-Suarez, Oxidative damage, bleomycin, and gamma radiation induce different types of DNA strand breaks in normal lymphocytes and thymocytes. A comet assay study, Ann. N. Y. Acad. Sci. 887 (1999) 133–149.
[15] N. Driessens, et al., Hydrogen peroxide induces DNA single- and double-strand breaks in thyroid cells and is therefore a potential mutagen for this organ, Endocr. Relat. Canc. 16 (3) (2009) 845–856.
[16] M. Valverde, et al., Hydrogen peroxide-induced DNA damage and repair through the differentiation of human adipose-derived mesenchymal stem cells, Stem Cell. Int. 2018 (2018) 1615497.
[17] S.P. Jackson, J. Bartek, The DNA-damage response in human biology and disease, Nature 461 (7267) (2009) 1071–1078.
[18] M. Valko, et al., Free radicals, metals and antioxidants in oxidative stress-induced cancer, Chem. Biol. Interact. 160 (1) (2006) 1–40.
[19] A. Matsuzawa, H. Ichijo, Redox control of cell fate by MAP kinase: physiological roles of ASK1-MAP kinase pathway in stress signaling, Biochim. Biophys. Acta 1780 (11) (2008) 1325–1336.
[20] P.J. Nadeau, et al., Disulfide Bond-mediated multimerization of Ask1 and its reduction by thioredoxin-1 regulate H(2)O(2)-induced c-Jun NH(2)-terminal kinase activation and apoptosis, Mol. Biol. Cell 18 (10) (2007) 3903–3913.
[21] Z. Guo, et al., ATM activation by oxidative stress, Science 330 (6003) (2010) 517–521.
[22] G. Giaccone, et al., Neuromedin B is present in lung cancer cell lines, Canc. Res. 52 (9 Suppl) (1992) 2732s–2736s.
[23] J. van den Berg, et al., A limited number of double-strand DNA breaks is sufficient to delay cell cycle progression, Nucleic Acids Res. 46 (19) (2018) 10132–10144.
[24] V.V. Pak, et al., Ultrasensitive genetically encoded indicator for hydrogen peroxide identifies roles for the oxidant in cell migration and mitochondrial function, Cell Metabol. 31 (3) (2020) 642–653, e6.
[25] J. Drost, et al., Sequential cancer mutations in cultured human intestinal stem cells, Nature 521 (7550) (2015) 43–47.
[26] A.C.F. Bolhaqueiro, et al., Ongoing chromosomal instability and karyotype evolution in human colorectal cancer organoids, Nat. Genet. 51 (5) (2019) 824–834.
[27] E. Kim, et al., Systematic functional interrogation of rare cancer variants identifies oncogenic alleles, Canc. Discov. 6 (7) (2016) 714–726.
[28] K.L. Meerbrey, et al., The pINDUCER lentiviral toolkit for inducible RNA interference in vitro and in vivo, Proc. Natl. Acad. Sci. U. S. A. 108 (9) (2011) 3665–3670.
[29] J.L. Hartley, G.F. Temple, M.A. Brasch, DNA cloning using in vitro site-specific recombination, Genome Res. 10 (11) (2000) 1788–1795.
[30] N. Vahsen, et al., AIF deficiency compromises oxidative phosphorylation, EMBO J. 23 (23) (2004) 4679–4689.
[31] X.R. Jiang, et al., Telomerase expression in human somatic cells does not induce changes associated with a transformed phenotype, Nat. Genet. 21 (1) (1999) 111–114.
[32] N.M. Mishina, et al., Which antioxidant system shapes intracellular H(2)O(2) gradients? Antioxidants Redox Signal. 31 (9) (2019) 664–670.
[33] H. Sies, D.P. Jones, Reactive oxygen species (ROS) as pleiotropic physiological signalling agents, Nat. Rev. Mol. Cell Biol. 21 (7) (2020) 363–383.
[34] M.A. Kang, et al., DNA damage induces reactive oxygen species generation through the H2AX-Nox1/Rac1 pathway, Cell Death Dis. 3 (2012) e249.
[35] J.M. Held, et al., Targeted quantitation of site-specific cysteine oxidation in endogenous proteins using a differential alkylation and multiple reaction monitoring mass spectrometry approach, Mol. Cell. Proteomics 9 (7) (2010) 1400–1410.
[36] Y. Cho, et al., Crystal structure of a p53 tumor suppressor-DNA complex: understanding tumorigenic mutations, Science 265 (5170) (1994) 346–355.
[37] M. Kitayner, et al., Structural basis of DNA recognition by p53 tetramers, Mol. Cell. 22 (6) (2006) 741–753.
[38] R. Rainwater, et al., Role of cysteine residues in regulation of p53 function, Mol. Cell Biol. 15 (7) (1995) 3892–3903.
[39] S.Y. Fuchs, et al., Mdm2 association with p53 targets its ubiquitination, Oncogene 17 (19) (1998) 2543–2547.
[40] Y. Haupt, et al., Mdm2 promotes the rapid degradation of p53, Nature 387 (6630) (1997) 296–299.
[41] K.Z. Guyton, et al., Activation of mitogen-activated protein kinase by H2O2. Role in cell survival following oxidant injury, J. Biol. Chem. 271 (8) (1996) 4138–4142.
[42] M. Hornsveld, et al., A FOXO-dependent replication checkpoint restricts proliferation of damaged cells, Cell Rep. 34 (4) (2021) 108675.
[43] E. Dickens, S. Ahmed, Principles of cancer treatment by chemotherapy, Surgery 36 (3) (2018) 134–138.
[44] S. Xie, et al., Reactive oxygen species-induced phosphorylation of p53 on serine 20 is mediated in part by polo-like kinase-3, J. Biol. Chem. 276 (39) (2001) 36194–36199.
[45] T.T. Paull, Mechanisms of ATM activation, Annu. Rev. Biochem. 84 (2015) 711–738.
[46] Y. Chen, et al., Collateral damage in cancer chemotherapy: oxidative stress in nontargeted tissues, Mol. Interv. 7 (3) (2007) 147–156.
[47] C. Yokoyama, et al., Induction of oxidative stress by anticancer drugs in the presence and absence of cells, Oncol Lett 14 (5) (2017) 6066–6070.
[48] D.J. Templeton, et al., Purification of reversibly oxidized proteins (PROP) reveals a redox switch controlling p38 MAP kinase activity, PloS One 5 (11) (2010), e15012.
[49] K.J. Nelson, et al., H(2)O(2) oxidation of cysteine residues in c-Jun N-terminal kinase 2 (JNK2) contributes to redox regulation in human articular chondrocytes, J. Biol. Chem. 293 (42) (2018) 16376–16389.
[50] S. Seemann, P. Hainaut, Roles of thioredoxin reductase 1 and APE/Ref-1 in the control of basal p53 stability and activity, Oncogene 24 (24) (2005) 3853–3863.
[51] J. Buzek, et al., Redox state of tumor suppressor p53 regulates its sequence-specific DNA binding in DNA-damaged cells by cysteine 277, Nucleic Acids Res. 30 (11) (2002) 2340–2348.
[52] S.W. Lowe, et al., p53 status and the efficacy of cancer therapy in vivo, Science 266 (5186) (1994) 807–810.
[53] A. Mandinova, S.W. Lee, The p53 pathway as a target in cancer therapeutics: obstacles and promise, Sci. Transl. Med. 3 (64) (2011) 64rv1.
[54] D. Yan, G. An, M.T. Kuo, C-Jun, N-terminal kinase signalling pathway in response to cisplatin, J. Cell Mol. Med. 20 (11) (2016) 2013–2019.
[55] A. Burgess, et al., Clinical Overview of MDM2/X-targeted therapies, Front Oncol 6 (2016) 7.
[56] S.E. Eriksson, et al., p53 as a hub in cellular redox regulation and therapeutic target in cancer, J. Mol. Cell Biol. 11 (4) (2019) 330–341.
[57] A. Glasauer, N.S. Chandel, Targeting antioxidants for cancer therapy, Biochem. Pharmacol. 92 (1) (2014) 90–101.
[58] Z. Zou, et al., Induction of reactive oxygen species: an emerging approach for cancer therapy, Apoptosis 22 (11) (2017) 1321–1335.
[59] C. Marzano, et al., Inhibition of thioredoxin reductase by auranofin induces apoptosis in cisplatin-resistant human ovarian cancer cells, Free Radic. Biol. Med. 42 (6) (2007) 872–881.
[60] A. Sobhakumari, et al., Susceptibility of human head and neck cancer cells to combined inhibition of glutathione and thioredoxin metabolism, PloS One 7 (10) (2012), e48175.
[61] M. Polimeni, et al., Modulation of doxorubicin resistance by the glucose-6-phosphate dehydrogenase activity, Biochem. J. 439 (1) (2011) 141–149.